PREDICTION OF THE OPERATING LIMITS OF REVOLVING HELICALLY GROOVED HEAT PIPES

Kevin S. Klasing[1] and Scott K. Thomas[2], Wright State University, Dayton, OH 45435
Kirk L. Yerkes[3], Wright–Patterson AFB, OH 45433–7251

Introduction

Revolving heat pipes have been proposed to be used for electric motor cooling and rotating heat exchangers (Thoren, 1984; Gi and Maezawa, 1990). Revolving heat pipes are defined herein as the case in which the axis of rotation is parallel to (but offset from) the central axis of the heat pipe. A literature survey has shown that most researchers utilized smooth–walled non–tapered revolving heat pipes because of their simplicity of manufacture (Thoren, 1984; Gi and Maezawa, 1990; Niekawa et al., 1981; Pokorny et al., 1984; Curtila and Chataing, 1984). However, smooth–walled heat pipes have not proven to be greatly effective because the working fluid is held against the outboard wall of the pipe, leaving a significant portion of the pipe wall dry. A remedy is to have large volumes of working fluid in the heat pipe, which increases the weight of the heat pipe and the potential for imbalance of the rotating system. In addition, it has been found that slight adverse tilt angles between the axis of rotation and horizontal, where the evaporator section is above the condenser section, can severely affect the performance of revolving non–tapered heat pipes. Another possibility is to install the heat pipe with a slight tilt (offset of the evaporator section from the axis of rotation is greater than that of the condenser section), such that the working fluid is forced back to the evaporator section due to the favorable body forces. However, this is not always possible due to the design of the machine to be cooled. Yet another alternative is to machine a slight taper on the interior of the pipe wall, but this severely limits the overall heat pipe length due to difficulties encountered in such a machining process. Therefore, a simple mechanism to reliably return the working fluid back to the evaporator section is needed. Recently, an experimental and analytical study was performed in which the capillary limit of a curved

[1]Graduate Research Assistant, Department of Mechanical and Materials Engineering
[2]Assistant Professor, Department of Mechanical and Materials Engineering
[3]Research Engineer, Air Force Research Laboratory (PRPG)

helically–grooved revolving heat pipe was found to increase with rotational speed (Thomas et al., 1998). This was due to the geometric nature of the helically–grooved wick structure. The helically–grooved copper tubing was found to be commercially available at a relatively low cost. The results of the aforementioned study (Thomas et al., 1998) has prompted the present analysis to determine the possibility of using helically–grooved straight heat pipes for the thermal management of rotating equipment.

Mathematical Model

A mathematical model was formulated to determine the operating limits of revolving helically–grooved heat pipes. The capillary limit calculation was complicated by the variation of the body force field along the length of the groove and around the circumference of the heat pipe. This required an analysis of the total body force imposed on the liquid along the length of the helical grooves. The boiling and entrainment limits were calculated using methods described by Faghri (1995).

Capillary Limitation. As shown in Figs. 1 and 2, the centerline of the heat pipe is parallel to and revolving about the z_1 axis at a radius R_p. The axis of rotation is tilted with respect to horizontal at an angle λ, where the evaporator is above the condenser. To find the total body force on the liquid, an inertial reference frame (x_1, y_1, z_1) is placed on the axis of rotation (Fig. 2). A non–inertial reference (x_2, y_2, z_2) is located at any point on the centerline of the helix. The (x_3, y_3, z_3) coordinate system is in the center of the helical groove at the same s location as the (x_2, y_2, z_2) system (Fig. 3). The x_3 unit vector is directed along the tangent to the helix, z_3 is directed toward the centerline, and y_3 is orthogonal to x_3 and z_3.

With respect to the liquid flow within the helical grooves, the following assumptions are made:

1. The grooves are completely filled along the length of the heat pipe with no puddling or depletion.

2. There is no communication of liquid between the grooves.

3. The liquid velocity vector is directed along the unit vector $\hat{e}_{x_3}$ (tangent to the helical groove).

4. Condensation and evaporation are uniform along the lengths of the condenser and evaporator sections, respectively.

These assumptions result in the following liquid velocity profile along the length of a groove (Silverstein, 1992)

$$\vec{V}_\ell = \begin{cases} \left\{ \left(\dfrac{s}{L_c} \right) V_{\ell,\max} \right\} \hat{\mathrm{e}}_{x_3} & 0 \le s < L_c \\ \{ V_{\ell,\max} \} \, \hat{\mathrm{e}}_{x_3} & L_c \le s < L_c + L_a \\ \left\{ \left(\dfrac{L_t - s}{L_e} \right) V_{\ell,\max} \right\} \hat{\mathrm{e}}_{x_3} & L_c + L_a \le s < L_t \end{cases} \tag{1}$$

Note that $V_{\ell,\max}$ is allowed to vary from one groove to another due to differences in the body forces between grooves. The velocity of the liquid $\vec{V}_\ell$ results in an angular velocity $\vec{\omega}_2$ of the (x_2, y_2, z_2) reference about the x_1 axis (Fig. 2). Since the helix angle α is constant, the angular velocity is

$$\vec{\omega}_2 = \left\{ \frac{R_p |\vec{V}_\ell| \sin\alpha}{R_p^2 + s^2} \right\} \hat{\mathrm{e}}_{x_1} \tag{2}$$

The liquid motion also results in an angular velocity $\vec{\omega}_3$ around the centerline of the helix, as shown in Fig. 3(b), due to the fluid path around the circumference of the heat pipe.

$$\vec{\omega}_3 = \left\{ \frac{|\vec{V}_\ell| \cos\alpha}{r_h} \right\} \hat{\mathrm{e}}_{z_2} \tag{3}$$

The acceleration vector at point P on the helix (Fig. 2) with respect to the inertial reference (x_1, y_1, z_1) is given by (Shames, 1980; Klasing et al., 1998)

$$\begin{aligned} \vec{A} = \left(\frac{d\vec{\omega}_3}{dt} \right) \times \vec{\rho} + \vec{\omega}_3 \times (\vec{\omega}_3 \times \vec{\rho}) + \left[\frac{d}{dt} (\vec{\omega}_1 + \vec{\omega}_2) \right] \times \vec{R} + (\vec{\omega}_1 + \vec{\omega}_2) \times [(\vec{\omega}_1 + \vec{\omega}_2) \times \vec{R}] \\ + 2(\vec{\omega}_1 + \vec{\omega}_2) \times (\vec{\omega}_3 \times \vec{\rho}) + \left[\frac{d}{dt} (\vec{\omega}_1 + \vec{\omega}_2) \right] \times \vec{\rho} + (\vec{\omega}_1 + \vec{\omega}_2) \times [(\vec{\omega}_1 + \vec{\omega}_2) \times \vec{\rho}] \end{aligned} \tag{4}$$

The position vectors $\vec{R}$ and $\vec{\rho}$ for a helical curve rotating about an offset vertical axis are

$$\vec{R} = \{R_p\} \hat{\mathrm{e}}_{y_1} + \{s\} \hat{\mathrm{e}}_{z_1} \tag{5}$$

$$\vec{\rho} = \{r_h \cos\phi\}\hat{e}_{x_1} + \{r_h \sin\phi\}\hat{e}_{y_1} \tag{6}$$

A pressure balance within the heat pipe results in the following expression for the capillary limit (Faghri, 1995; Chi, 1976).

$$\Delta P_{\text{cap,max}} \geq \Delta P_v + \Delta P_\ell + \Delta P_{\text{bf}} \tag{7}$$

The maximum capillary pressure is

$$\Delta P_{\text{cap,max}} = \frac{2\sigma}{r_c} \tag{8}$$

where the capillary radius is equal to the helical groove width $r_c = w$. For a circular cross section of a heat pipe with uniform heat input and output along the lengths of the evaporator and condenser, respectively, the pressure drop in the vapor is

$$\Delta P_v = \frac{4\mu_v Q_t}{\pi \rho_v h_{\text{fg}} r_v^4} \left(L_e + 2L_a + L_c\right) \tag{9}$$

The liquid pressure drop within a particular groove is (Klasing, 1998)

$$\Delta P_\ell = \int_0^{L_g} \frac{\mu_\ell \dot{m}_\ell}{\rho_\ell A_w K}\, dx_3 = \frac{\mu_\ell Q_g \left(f\text{Re}\right)_\ell \left(L_e + 2L_a + L_c\right)}{4\rho_\ell r_\ell^2 w h h_{\text{fg}}} \sqrt{\left(\frac{2\pi r_h}{p}\right)^2 + 1} \tag{10}$$

The coefficient of drag within a rectangular groove is given by (Shah and Bhatti, 1987)

$$\left(f\text{Re}\right)_\ell = 24(1 - 1.3553\beta + 1.9467\beta^2 - 1.7012\beta^3 + 0.9564\beta^4 - 0.2537\beta^5) \tag{11}$$

where the range of the aspect ratio is $0 \leq \beta \leq 1$.

The total body force imposed on the fluid within a particular groove may either aid or hinder the return of the fluid to the evaporator, depending on the groove pitch p, the angle of the starting point of the helix ϕ_0, the rotational speed, and the inclination angle. However, even if the body force hinders the return of the fluid, each groove contributes to the total heat transported. Therefore, the capillary limit equation [eqn. (7)] was first solved for the

heat transported by each individual groove Q_g, and the results were summed to determine the total heat transport Q_t. Since the pressure drop in the vapor space was a function of the total heat transported, eqn. (7) was solved iteratively.

For a given tilt angle λ (see Fig. 1), the body force due to gravity in the tangent direction has a changing magnitude as the pipe revolves with constant angular velocity $\vec{\omega}_1$. Since the objective of this analysis was to find the steady–state capillary limit, it was necessary to find the average value of the body force due to gravity in the tangent direction ($\hat{\mathrm{e}}_{x_3}$) for a single revolution. The body forces in the tangent direction due to acceleration [eqn. (4)] and gravity were integrated over the length of the groove to find the average pressure drop due to body forces

$$\Delta P_{\mathrm{bf}} = -\rho_\ell \sqrt{\left(\frac{2\pi r_h}{p}\right)^2 + 1} \left[\int_0^{L_t} \hat{\mathrm{e}}_{x_3} \cdot \left(-\vec{A}\right)\, ds + \frac{1}{2\pi\rho_\ell} \int_0^{L_t} \int_0^{2\pi} \hat{\mathrm{e}}_{x_3} \cdot \vec{F}_g \, d\theta \, ds \right] \tag{12}$$

where the body force per unit volume due to gravity is

$$\vec{F}_g = \{\rho_\ell g \cos\lambda\}\, \hat{\mathrm{e}}_{y_1} + \{-\rho_\ell g \sin\lambda\}\, \hat{\mathrm{e}}_{z_1} \tag{13}$$

The general expression for the maximum capillary limit for a single groove is

$$\begin{aligned} \frac{2\sigma}{w} \geq \frac{(L_e + 2L_a + L_c)}{h_{\mathrm{fg}}} & \left\{ \frac{4\mu_v Q_t}{\pi\rho_v r_v^4} + \frac{\mu_\ell Q_g \,(f\mathrm{Re})_\ell}{4\rho_\ell r_\ell^2 w h} \sqrt{\left(\frac{2\pi r_h}{p}\right)^2 + 1} \right\} \\ & -\rho_\ell \sqrt{\left(\frac{2\pi r_h}{p}\right)^2 + 1} \left[\int_0^{L_t} \hat{\mathrm{e}}_{x_3} \cdot \left(-\vec{A}\right)\, ds + \frac{1}{2\pi\rho_\ell} \int_0^{L_t} \int_0^{2\pi} \hat{\mathrm{e}}_{x_3} \cdot \vec{F}_g \, d\theta \, ds \right] \end{aligned} \tag{14}$$

This equation was solved for each individual groove. However, the total heat transported Q_t was not known *a priori*, so an iterative solution procedure was necessary.

To quantify the assumption of no communication of liquid between the grooves, the Bond number was used, which was defined as

$$\mathrm{Bo} = \frac{\rho_\ell\, r_\ell |\vec{A}_{\mathrm{res}}|}{2\sigma/w} = \frac{\text{Body Force}}{\text{Surface Tension Force}} \tag{15}$$

where $\vec{A}_{\text{res}}$ is the resultant acceleration vector between the y_3 and z_3 directions.

Boiling Limitation. The formation of bubbles (nucleation) within the wick structure of a heat pipe can adversely affect its performance. The growth and motion of bubbles within the wick structure can effectively shut off the liquid return path, causing dryout of the evaporator. The boiling limitation corresponding to a cylindrical heat pipe is (Faghri, 1995)

$$Q_b = \frac{2\pi L_e k_{\text{eff}} \Delta T_{\text{crit}}}{\ln\left(r_i/r_v\right)} \tag{16}$$

The effective thermal conductivity in the evaporator section for grooved heat pipe wick structures is (Chi, 1976)

$$k_{\text{eff}} = \frac{L k_\ell k_s h + w k_\ell \left(0.185 L k_s + h k_\ell\right)}{\left(w + L\right)\left(0.185 L k_s + h k_\ell\right)} \tag{17}$$

The critical temperature difference between the heat pipe wall and the vapor is given by

$$\Delta T_{\text{crit}} = \frac{2\sigma T_a}{h_{\text{fg}} \rho_v} \left(\frac{1}{R_b} - \frac{1}{r_c}\right) \tag{18}$$

Since experimental data is not available for axially–grooved heat pipes, the value suggested by Faghri (1995) for the nucleation bubble radius was used ($R_b = 10^{-7}$ m).

Entrainment Limitation. The entrainment limit is caused by the viscous interaction of the vapor and liquid flows in the wick structure. Droplets of liquid within the wick structure may be entrained into the counterflowing vapor and carried back to the condenser end cap before reaching the evaporator section, effectively shutting off the liquid flow and drying out the evaporator section. For an axially–grooved heat pipe, the entrainment limitation is given by (Faghri, 1995)

$$Q_e = A_v h_{\text{fg}} \left(\frac{\sigma \rho_v}{2w}\right)^{1/2} \tag{19}$$

The temperature dependence of the thermophysical properties was accounted for using the polynomial curve fits (evaluated at the adiabatic temperature) given by Faghri (1995). The heat transfer in the circumferential and axial directions through the pipe wall was neglected in the present model.

Table 1: Heat pipe specifications.

Wick structure	Helical grooves
Working fluid	Water
Heat pipe length, L_t	457.2 mm
Evaporator length, L_e	152.4 mm
Adiabatic length, L_a	101.6 mm
Condenser length, L_c	152.4 mm
Vapor core diameter, D_v	13.46 mm
Wall/wick materials	Copper
Helix pitch, p	914.4 mm CW
Groove height, h	0.44 mm
Groove width, w	0.47 mm
Number of grooves, N_g	50

Results and Discussion

The specifications of the heat pipe studied in this analysis is given in Table 1. The heat pipe analyzed was similar to that presented by Thomas et al. (1998), who found that the capillary limit was maximized when $p/L_t = 2$. In the present study, this optimized pitch specification was assumed in the analysis to examine the operating characteristics of straight helically–grooved heat pipes. It should be noted that the Bond number was less than unity for all results reported. Water was chosen as the working fluid to accomodate a wide range of temperatures above ambient.

The maximum heat transport versus working (adiabatic) temperature for rotational speeds of 0, 250 and 500 RPM is shown in Fig. $4(a)$. The boiling limit decreased with temperature, while the entrainment limit increased with temperature. In the present analysis, the boiling and entrainment limits are independent of the rotational speed. As can be seen, the capillary limit increased significantly with rotational speed due to the helical geometry of the heat pipe wick structure. It should be noted that the maximum heat transport is defined as the lowest limit value for a given temperature. For instance, for $\vec{\omega}_1 = 0$, the capillary limit determined the heat pipe performance between $T_a = 100°\text{C}$ and approximately $T_a = 133°\text{C}$, and the boiling limit was in effect for $T_a > 133°\text{C}$. Over the range of temperature examined, the heat pipe was not limited by capillary effects for rotational

speeds of $\vec{\omega}_1 = 500$ RPM for the case shown in Fig. $4(a)$.

The variation of the maximum heat transport versus tilt angle is shown in Fig. $4(b)$. For a stationary heat pipe ($\vec{\omega}_1 = 0$ RPM), the capillary limit decreased from over $Q_{\text{cap}} = 1000$ W to zero as the tilt angle ranged from $\lambda = 0°$ to $4°$. This type of behavior was observed experimentally by Faghri and Thomas (1989), who studied a stationary axially–grooved copper–water heat pipe. In general, the maximum heat transport increased with rotational speed. For $\vec{\omega}_1 = 500$ and 750 RPM, the heat pipe was restricted by the entrainment limit or capillary limit, depending on the tilt angle.

The variation of the maximum heat transport versus rotational speed is shown in Fig. $4(c)$. For the horizontal case ($\lambda = 0°$), the capillary limit was constant for $\vec{\omega}_1 < 200$ RPM. For rotational speeds above $\vec{\omega}_1 = 200$ RPM, the capillary limit increased until the entrainment limit was reached. For $\lambda = 90°$, the heat pipe did not operate at all until a rotational speed above approximately $\vec{\omega}_1 = 700$ RPM was reached. This shows that a minimum value of rotational speed was needed to obtain the benefits of the helical groove geometry. For rotational speeds greater than $\vec{\omega}_1 \simeq 900$ RPM, the heat pipe was not limited by capillary effects.

Conclusions

The performance of a helically–grooved revolving heat pipe has been examined for various working temperatures, adverse tilt angles, and rotational speeds. It was determined that the capillary limit increased significantly with rotational speed due to the helical geometry of the heat pipe wick structure. A minimum value of rotational speed was required to obtain the benefits of the helical groove geometry when an adverse tilt angle was imposed on the heat pipe. Unlike smooth–walled non–tapered revolving heat pipes, the helical groove wick structure allows the present heat pipe to operate when the adverse tilt angle is $\lambda = 90°$ under certain conditions. While these results are promising in regard to applying helically–grooved heat pipes to the thermal management of rotating equipment, experimental data is needed to verify the findings of the model described herein.

Nomenclature

A_v	cross–sectional area of the vapor space, m

A_w	cross–sectional area of the wick, $\pi h\,(2r_v + h)$, m^2
$h_{\rm fg}$	heat of vaporization, J/kg
k_ℓ	liquid thermal conductivity, W/(m-K)
k_s	solid wick material thermal conductivity, W/(m-K)
K	permeability, $2\epsilon r_\ell^2/(f_\ell {\rm Re}_\ell)$, m^2
L	distance between grooves, m
L_g	groove length, m
$\dot{m}$	mass flow rate, kg/s
r_h	radius of the helix, $r_v + h/2$, m
r_i	inner wall radius of the heat pipe, m
r_ℓ	liquid hydraulic radius, $2wh/(2h + w)$, m
r_v	radius of the heat pipe vapor space, m
s	coordinate along the centerline of the helix, m
$V_{\ell,\max}$	liquid velocity in the adiabatic section, $Q_g/\rho_\ell whh_{\rm fg}$, m/s
β	aspect ratio, w/h
ϵ	porosity, whN_g/A_w
μ	absolute viscosity, kg/(m-s)
ρ	density, kg/m^3
σ	surface tension, N/m
ϕ	angular parameter, $\phi_0 + 2\pi s/p$, rad

References

Chi, S., 1976, *Heat Pipe Theory and Practice: A Sourcebook,* Hemisphere Publ. Corp., New York.

Curtila, R., and Chataing, T., 1984, "Experimental Study of a Revolving Heat Pipe," *Proceedings of the 5th International Heat Pipe Conference*, pp. 268–273, Tsukuba, Japan.

Faghri, A., 1995, *Heat Pipe Science and Technology,* Taylor and Francis, Washington, DC.

Faghri, A., and Thomas, S., 1989, "Performance Characteristics of a Concentric Annular Heat Pipe: Part I—Experimental Prediction and Analysis of the Capillary Limit," ASME J. Heat Transfer, Vol. 111, pp. 844–850.

Gi, K., and Maezawa, S., 1990, "Heat Transfer Characteristics of a Parallel Rotating Heat Pipe," *Proceedings of the 7th International Heat Pipe Conference*, pp. 271–283, Minsk, Belarus.

Klasing, K. S., 1998, "Performance Characteristics of Revolving Helically–Grooved Heat Pipes," Master's Thesis, Wright State University, Dayton, OH.

Klasing, K., Thomas, S., and Yerkes, K., 1998, "Prediction of the Operating Limits of Revolving Helically Grooved Heat Pipes," *Proceedings of the ASME/AIAA Joint Thermophysics Conference,*" HTD-Vol. 357-3, pp. 117–128, Albuquerque, NM.

Niekawa, J., Matsumoto, K., Koizumi, T., Hasegawa, K., Kaneko, H., and Mizoguchi, Y., 1981, "Performance of Revolving Heat Pipes and Application to a Rotary Heat Exchanger," *Proceedings of the 4th International Heat Pipe Conference*, pp. 225–234, London.

Pokorny, B., Polasek, F., Schneller, J., and Stulc, P., 1984, "Heat Transfer in Co–Axial and Parallel Rotating Heat Pipes," *Proceedings of the 5th International Heat Pipe Conference*, pp. 259–267, Tsukuba, Japan.

Shah, R.K., and Bhatti, M.S., 1987, "Laminar Convective Heat Transfer in Ducts," in *Handbook of Single–Phase Convective Heat Transfer*, Eds., Kakac, S., Shah, R.K., and Aung, W., Wiley, New York.

Shames, I., 1980, *Engineering Mechanics*, 3rd Edn., Prentice–Hall, New Jersey.

Silverstein, C., 1992, *Design and Technology of Heat Pipes for Cooling and Heat Exchange*, Taylor & Francis, Washington, DC.

Thomas, S., Klasing, K., and Yerkes, K., 1998, "The Effects of Transverse Acceleration–Induced Body Forces on the Capillary Limit of Helically Grooved Heat Pipes," *ASME J. Heat Transfer*, Vol. 120, pp. 441–451.

Thoren, F., 1984, "Heat Pipe Cooled Induction Motors," *Proceedings of the 5th International Heat Pipe Conference*, pp. 365–371, Tsukuba, Japan.

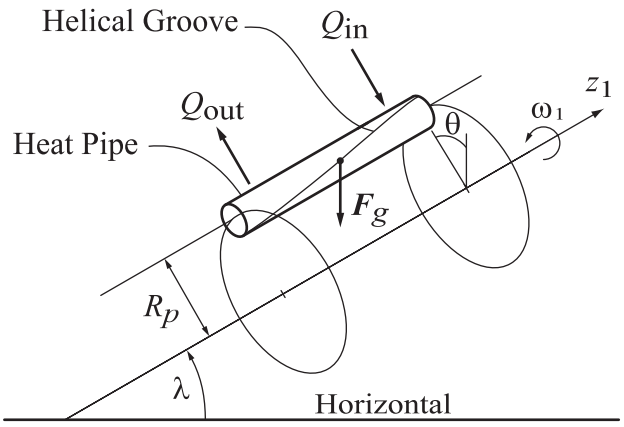

Figure 1: Schematic of the revolving helically–grooved heat pipe.

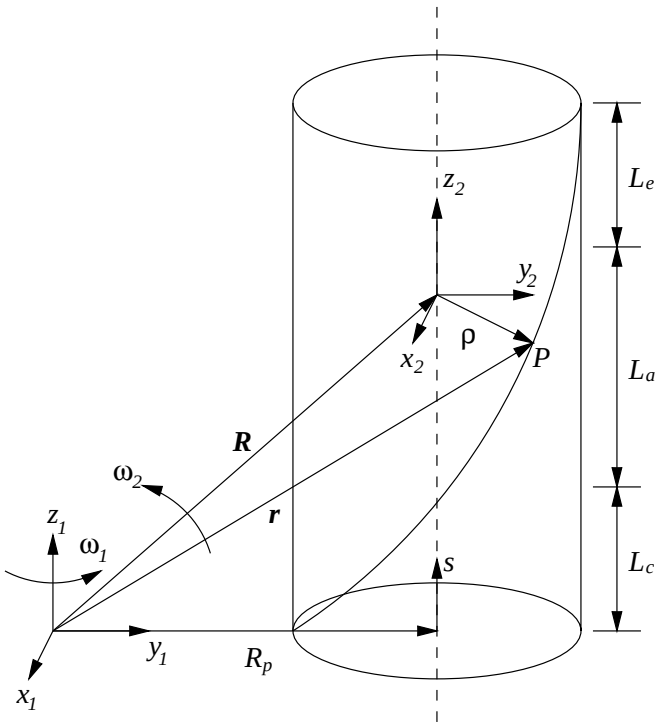

Figure 2: Relationships between vectors and reference frames.

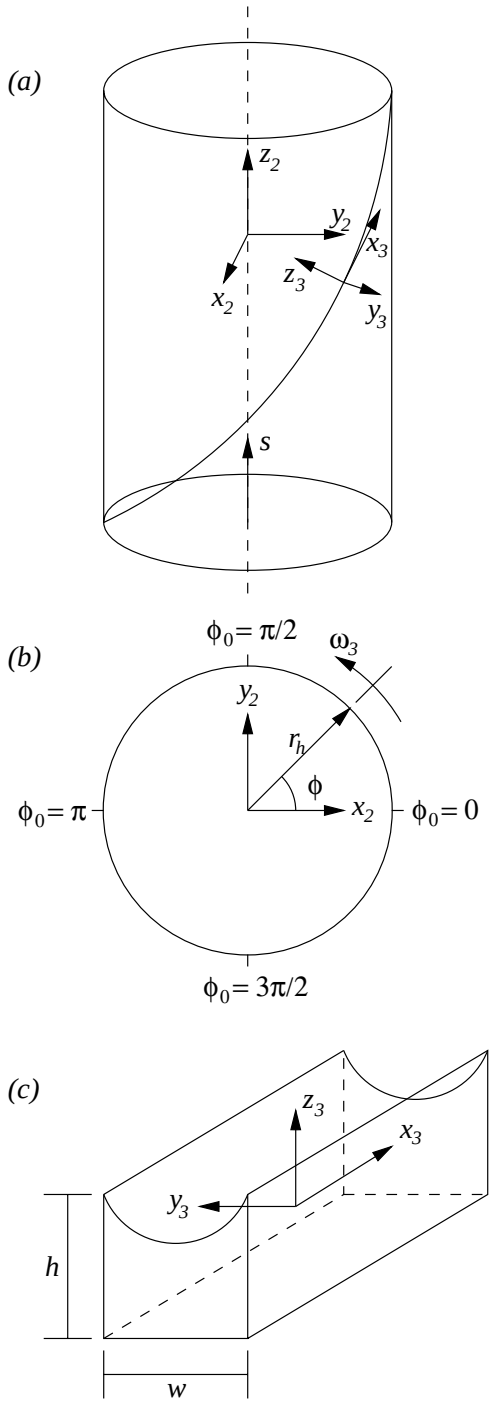

Figure 3: Geometric considerations: (a) Relationship between (x_2, y_2, z_2) and (x_3, y_3, z_3); (b) Cross–sectional view of the heat pipe at a particular s location; (c) Coordinate system situated in the helical groove.

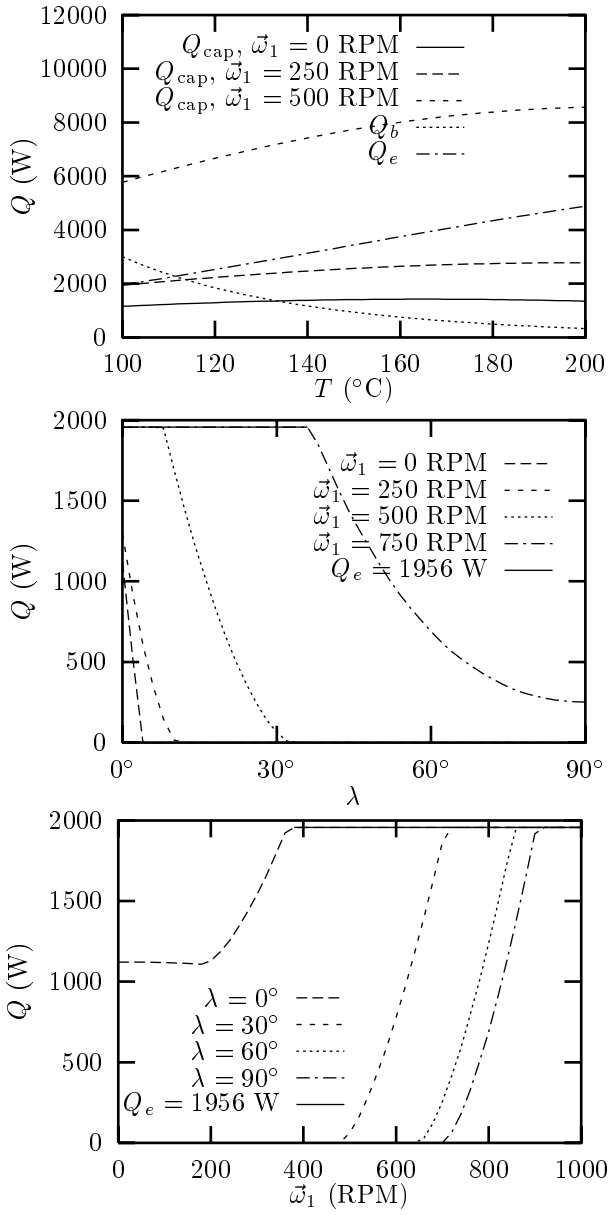

Figure 4: Heat transport limitation versus: (a) Working temperature ($\lambda = 0°$, $R_p = 0.1$ m); (b) Tilt angle ($T_a = 100°$C, $R_p = 0.05$ m); (c) Rotational speed ($T_a = 100°$C, $R_p = 0.05$ m).